2010 3rd International Conference on Computer and Electrical Engineering (ICCEE 2010)
IPCSIT vol. 53 (2012) © (2012) IACSIT Press, Singapore
DOI: 10.7763/IPCSIT.2012.V53.No.1.74

Noise Analysis for Active CMOS Mixers Including Memory Effect

Benqing Guo[1+], Guangjun Wen[1] and Xiaolei Li[2]

[1]Department of Communication Engineering, UESTC, Chengdu, China
[2]School of Electronic Engineering, UESTC, Chengdu, China

Abstract. A simple approach based on linear periodic time-varying theory, is developed to analyze the noise characteristics of active CMOS mixers. Based on the derived transfer functions with memory effect, the frequency-dependent noise transforming factors for individual stages in the mixers are numerically computed to rigorously describe the noise output. A unified noise expression considering both the thermal noise and the flicker noise is presented, and verified by simulations.

Keywords: CMOS mixers; noise; memory effect; time-varying

1. Introduction

Direct conversion receivers (DCR) with the advantage of low cost and high integration, have gained more increased commercial market quotient among various receiver architectures. For DCR, not only thermal noise from mixers, but also flicker noise can seriously deteriorate the overall system performance. On the other hand, the active mixer is more attractive in many applications because it provides higher conversion gain, resulting in improved suppression of noise contribution from subsequent stages. Therefore it is undoubtedly significant to accurately analyze and predict the noise characteristics of active mixers [1-4].

Efforts to understand noise in mixers on a more intuitive basis have resulted in a few analytical methods [3-4], but the memory elements such as capacitors are commonly ignored. Hence, the existing analytical approaches provide rather limited design insights when LO frequency is high. In this work, a simple approach based on linear periodic time-varying theory [5], is developed to analyze the noise characteristics of the mixer, incorporating memory effect. The proposed analysis approach is a generalization for [3], and ultimately validated by simulations.

The paper is organized as follows. In section Ⅱ, the noise analysis for the mixer is presented through deriving corresponding periodic transfer function. And in section Ⅲ, simulations verify the theory. Finally, conclusions are drawn in section Ⅳ.

2. Noise analysis

Without losing generality, the single balanced CMOS active mixer shown in Fig.1 is examined. It is composed of an input transconductance stage (M_3), switching pairs (M_1 and M_2), and output loads (R_L). In principle, M_1 and M_2 commutate the tail current I_3 under the control of LO signal $V_{LO}(t)$ and complete the frequency transformation from the RF to the IF, while M_3 converts the RF voltage signal v_{RF} to the current i_{RF}. The noise is contributed by all the devices in theory. Based on the derived transfer functions with the parasitic Cp, the frequency-dependent noise characteristic in the mixer is systematically analyzed throughout this section.

+ Corresponding author.
E-mail address: benqingguo@hotmail.com.

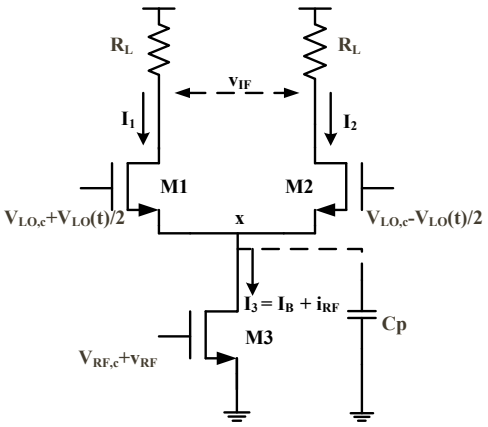

Figure 1. Single balanced CMOS active mixer.

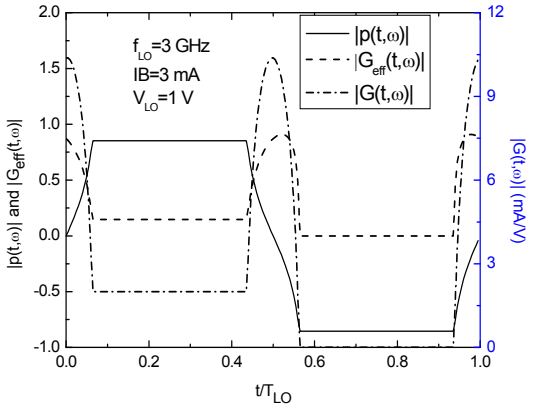

Figure 2. |P(t,ω)|, |Geff(t,ω) |, and |G(t,ω) | in TLO when IB=3 mA, VLO=1V, fLO=3 GHz

2.1 Noise from the transconductance stage

By small signal analysis, the fundamental transfer function from the RF port to the IF port, takes the form

$$P(t,\omega)=\frac{g_{m1}-g_{m2}}{g_{m1}+g_{m2}+j\omega C_p} \tag{1}$$

where parameter $g_{m1,2}$ is transconductance of $M_{1,2}$, and can be iteratively solved by switching pairs' equation [3]. P(t,ω) is periodic since $g_{m1,2}$ is time-varying in one LO period, T_{LO}. What's more, in fact, it also can be obtained by solving differential equations in time domain, and is omitted due to the limited space. According to cyclostationary theory [2], we have

$$P^{(n)}(\omega)=\frac{1}{T_{LO}}\int_0^{T_{LO}} P(t,\omega-n\omega_{LO})\exp(-jn\omega_{LO}t)\,dt \ . \tag{2}$$

As a result, the conversion gain of the single balanced mixer is

$$g_c=c(\omega)\cdot g_{m3}R_L \tag{3}$$

where parameter c(ω) and g_{m3} donate the switching pairs gain coefficient and transconductance for M_3. It can be seen that the equation $c(\omega_{IF})= |p^{-1}(\omega_{IF})|$ donates down conversion. When LO signal frequency f_{LO} is high enough (supposing f_{IF} near to zero), RF signal will be inevitably attenuated by the parasitic Cp. In other words, as shown in Fig.2, the transfer function p(t,ω) is lowered, and the waveform amplitude of that is even less than one. So c(ω) is decreased correspondingly. Fig.3 displays the relation of c(ω) vs. the bias current I_B with different f_{LO}.

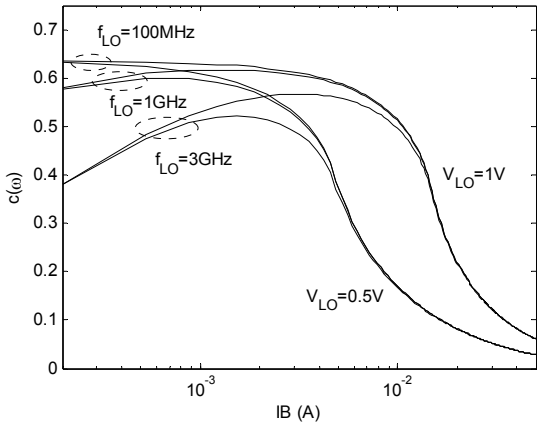

Figure 3. Numerically computed gain coefficient c(ω)

In transconductance stage, the noise sources include the thermal channel noise current of M_3, the input source resistance R_s and the polysilicon gate resistance r_{g3}. According to the cyclostationary principle, the noise power spectral density (PSD) transformed to the output due to the wide-sense-stationary (WSS) noise input at the transconductance stage is

$$S_{n3}^{o}(\omega)=\sum_{n=-\infty}^{\infty}\left|P^{(n)}(\omega)\right|^2\cdot 4kT\left(R_s+r_{g3}+\frac{\gamma}{g_{m3}}\right)g_{m3}^2 \tag{4}$$

where γ is the noise coefficient of devices. And we also define the noise transforming factor of transconductance stage $\alpha(\omega)=\sum|p(\omega)|^2$. As shown in Fig.4, high f_{LO} will decrease the numerical value of α(ω), which is similar to c(ω).

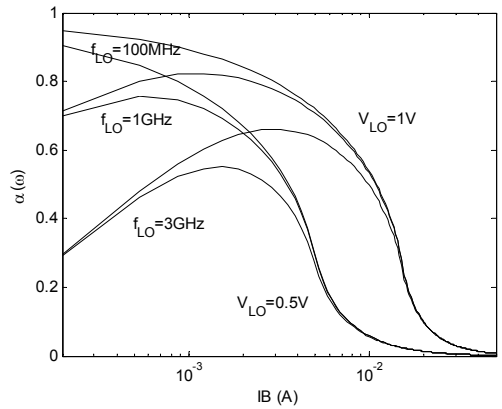

Figure 4. Numerically computed transforming factor α(ω)

2.2 Noise from the LO port resistance

Without loss of generality, the noise of LO Port resistance at the gate of M_1 is firstly considered. Similarly, the periodic transfer function from the LO port at M_1 side to IF port, takes the form

$$G(t,\omega)=\frac{g_{m1}\left(2g_{m2}+j\omega C_p\right)}{g_{m1}+g_{m2}+j\omega C_p}\ . \tag{5}$$

Considering the symmetry of switching pairs, the noise contribution to the output at LO port is

$$S_{nLO}^{o}(\omega)=\sum_{n=-\infty}^{\infty}\left|G^{(n)}(\omega)\right|^2 4kT(R_{LO}+2r_{g1}) \tag{6}$$

where R_{LO}, r_{g1} are the equivalent noise resistance of LO port, and the polysilicon gate resistance of M_1. And we also define the noise transforming factor of switching pairs $\beta(\omega)=\sum|G(\omega)|^2$. Similarly, we can have

$$G^{(n)}(\omega)=\frac{1}{T_{LO}}\int_0^{T_{LO}}G(t,\omega-n\omega_{LO})\exp(-jn\omega_{LO}t)\,dt\ . \tag{7}$$

The periodic waveform in T_{LO} for the transfer function |G(t,ω)| is also exemplified in Fig.2 with the typical I_B=3mA ,V_{LO}=1 V, and f_{LO}=3 GHz. Fig.5 depicts the relation of β(ω) vs. I_B with different f_{LO}.

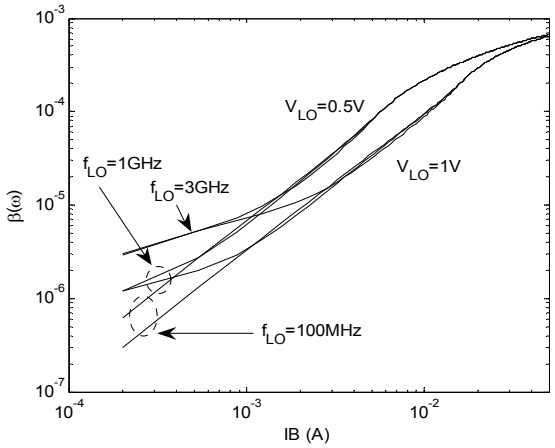

Figure 5. Numerically computed transforming factor of LO port at M1 side β(ω)

2.3 Noise from switching transistors

For the channel noise of switching transistors, the conclusion for WSS input in [2] can not be directly applied because the channel noise source of switching transistors behaviors cyclostationary. Fortunately, the cyclostationary noise source can be modeled as modulated stationary noise sources. And the modulated effect can be incorporated in the periodic transfer function. Still take M_1 for example, its cyclostationary noise $4kT\gamma g_{m1}$ is modeled as a WSS noise $4kT\gamma g_{m1max}$ modulated by a periodic waveform with normalized amplitude g_{m1}/g_{m1max}(g_{m1max} being the maximum of g_{m1} in T_{LO}). The corresponding effective periodic transfer function with modulated effect, thus takes the form

$$G_{\text{eff}}(t,\omega)=\sqrt{\frac{g_{m1}}{g_{m1,\max}}}\,\frac{2g_{m2}+j\omega C_p}{g_{m1}+g_{m2}+j\omega C_p}\ . \tag{8}$$

As a result, the noise PSD contribution to the output due to M_1 is

$$S^{o}_{\text{n1,wte}}(\omega)=\sum_{n=-\infty}^{\infty}\left|G^{(n)}_{eff}(\omega)\right|^2 4KT\gamma\cdot g_{m1,\max}\ . \tag{9}$$

And we also define the effective noise transforming factor of switching pairs $\beta_{eff}(\omega)=\sum|G_{eff}(\omega)|^2$. Then we also have

$$G^{(n)}_{eff}(\omega)=\frac{1}{T_{LO}}\int_0^{T_{LO}} G_{eff}(t,\omega-n\omega_{LO})\exp(-jn\omega_{LO}t)\,dt \tag{10}$$

The periodic waveform of transfer function $|G_{eff}(t,\omega)|$ in T_{LO} is also quantitatively depicted in Fig.2 with the same I_B=3mA,V_{LO}=1 V, and f_{LO}=3 GHz. As shown in Fig.6, high f_{LO} will decrease the numerical value of effective noise transforming factor of switching pairs $\beta_{eff}(\omega)$, which is similar to β(ω).

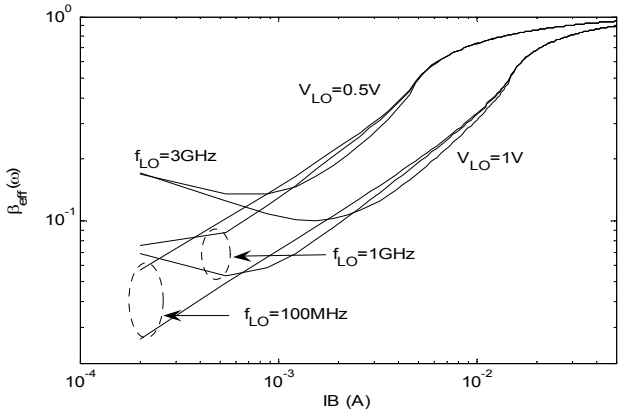

Figure 6. Numerically computed effective transforming factor βeff(ω)

2.4 Flicker Noise

The flicker noise of the mixer exclusively arises from the leakage from switching pairs $M_{1,2}$ [3-4]. The flicker noise output PSD due to M_1 can be expressed as follows

$$S^o_{n1,flk}(\omega) = \left|G^{(0)}(\omega)\right|^2 \overline{V^2_{n1}} \quad . \tag{11}$$

where parameter $G^{(0)}(\omega)$ is the time-average of transfer function $G(t,\omega)$ in T_{LO}, and can be obtained according to (7). Moreover, the flicker noise of M_1 is

$$\overline{V^2_{n1}} = \frac{K_f}{C_{OX} W_1 L} \frac{1}{f} \tag{12}$$

where parameter K_f is a process parameter. This model is not as accurate as the BSIM3v3 model, but serves as analytical formulation and has been used extensively to model flicker noise for the first-order approximate solutions.

2.5 Noise Figure

Based on the noise contributions in above, with the symmetry of switching pairs, the single sideband (SSB) noise figure (NF) for the single balanced mixer is

$$NF = \frac{S^o_{n3}(\omega) + 2S^o_{n1,wte}(\omega) + 2S^o_{n1,flk}(\omega) + S^o_{nLO}(\omega) + S^o_{nRL}}{c(\omega)^2 g^2_{m3} 4kTR_s} \tag{13}$$

where the noise from the loads R_L , S_{nRL} is

$$S^o_{nRL} = 8kT/R_L \quad . \tag{14}$$

This noise expression is unified in that it consists of not only the thermal noise but also the flicker noise. If f_{IF} is high enough to make the flicker noise close to zero, (13) reduces to the expression (43) in [3]. Only by computing several frequency-dependent transfer functions, the noise characteristic of the mixer can be conveniently predicted even if f_{LO} is high.

3. Simulated results and discussions

To validate this theory, the single balanced mixer shown in Fig.1, is simulated using Spectre-RF based on Chartered 0.35 μm process. $M_{1,2}$ and M_3 are sized with 100 μm /0.35 μm and 80 μm/0.35 μm. Especially, the simulated parasitic Cp is about 300fF, which includes the switch parasitic capacitance, output capacitance of the transconductance stage. And the noise coefficient for short channel devices approximately takes 2.5[6].

Here, take f_{IF}=100 kHz for example to analysis the noise in DCR, the noise and conversion gain character is compared between simulations and predications with the typical V_{LO} =0.5, 1 V and f_{LO} =1, 3 GHz respectively. Take V_{LO}=1 V for example, it's interesting that the simulated optimum noise figure is about 11.91 dB at I_B= 1.6 mA for f_{LO} =1 GHz while it takes 12.68 dB or so at I_B=2.1 mA for f_{LO} =3 GHz. The reason for this phenomenon lies in that the decreased $c(\omega)$, $\alpha(\omega)$ and increased $\beta(\omega)$, $\beta_{eff}(\omega)$ are respectively resulted in and responsible to the deterioration of noise figure when f_{LO} gets higher. Then it's no wonder that the simulated optimum conversion gain is reduced with f_{LO} getting higher.

On the whole, the simulated noise and conversion gain well agrees with the predictions even when f_{LO} becomes as high as 3 GHz. The NF discrepancy between simulations and predictions mainly lies in that parameter γ is in fact not solely dependent on channel length of devices, but related to bias current, drain and body voltage of devices [7]. For example, a recent research indicates that the low current density generally yields a small γ [8].

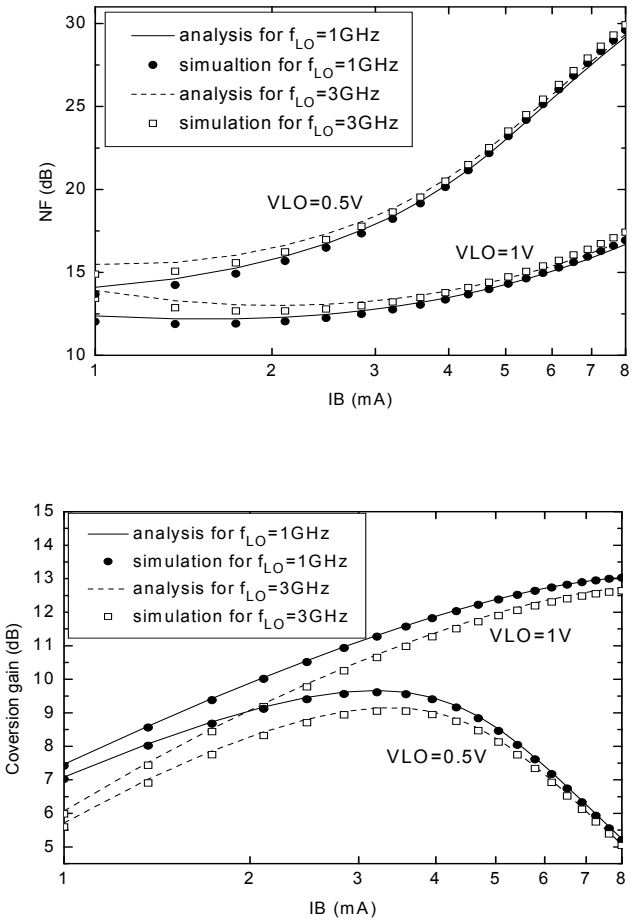

Figure 7. NF and conversion gain vs. IB at fIF= 100 kHz

4. Conclusions

A simple approach based on linear periodic time-varying theory is developed to analyze the noise characteristics of active CMOS mixers. Based on the derived transfer functions with memory effect, the frequency-dependent noise transforming factors for individual stages in the mixers are numerically computed to rigorously describe the noise output. A unified noise figure expression including both the thermal noise and the flicker noise has been proposed and is of great competency in the noise prediction of the mixer particularly when LO frequency is high.

5. Acknowledgment

The authors would like to thank Prof. Jianguo Ma in Tianjin University for ever helpful discussions and advices.

6. References

[1] Roychowdhury, J., "Cyclostationary noise analysis of large RF circuits with multitone excitations," IEEE J. Solid-State Circuits, vol. 33, pp.324-335, 1998.

[2] C. D. Hull and R. G. Meyer, "A systematic approach to the analysis of noise in mixers," IEEE Trans. Circuits Syst. I, vol. 40, pp. 909-919, 1993.

[3] M. T. Terrovitis and R. G. Meyer, "Noise in current-commutating CMOS mixers," IEEE J. Solid-State Circuits, vol. 34, pp. 772-783, 1999.

[4] H. Darabi and A. A. Abidi, “Noise in RF-CMOS mixers: A simple physical model,” IEEE J. Solid-State Circuits, vol. 35, pp. 15-25, 2000.

[5] W. A. Gardner, Introduction to Random Processes with Applications to Signals and Systems, 2nd ed., New York: McGraw-Hill, 1989.

[6] T. H. Lee, The Design of CMOS Radio-Frequency Integrated Circuits, 2nd ed., New York: Cambridge University Press, 2004.

[7] Y. Tsividis, Operation and modeling of the MOS transistor, McGraw-Hill, 1999.

[8] Zhiyuan Li and Jianguo Ma, “Compact channel noise models for deep-submicron mosfet,” IEEE trans. Electron devices, vol. 56, pp.1300-1307, 2009.